

# Investigations of the Residual Stresses and Surface Integrity Generated by a Novel Mechanical Surface Strengthening

Dennise Tanoko Ardi<sup>1, a\*</sup>, Wang Wei<sup>1, b</sup>, Iain Parr<sup>2, c</sup>, Goetz Feldmann<sup>3, d</sup>,  
Ampara Aramcharoen<sup>4, e</sup>, Chow Cher Wong<sup>4, f</sup>

<sup>1</sup>Advanced Remanufacturing and Technology Centre, 3 Cleantech Loop #01-01, Singapore 637143, Singapore

<sup>2</sup>Rolls-Royce Plc, ELT-10, PO Box 31, Derby DE24 8BJ, United Kingdom

<sup>3</sup>Rolls-Royce Deutschland Ltd & Co KG, Hohemarkstraße 60-70, 61440 Oberursel, Germany

<sup>4</sup>Rolls-Royce Singapore, Advanced Technology Centre, 1 Seletar Aerospace Crescent, Singapore 797565, Singapore

<sup>a\*</sup> [denniseta@artc.a-star.edu.sg](mailto:denniseta@artc.a-star.edu.sg), <sup>b</sup> [wangwei@artc.a-star.edu.sg](mailto:wangwei@artc.a-star.edu.sg), <sup>c</sup> [iain.parr@rolls-royce.com](mailto:iain.parr@rolls-royce.com),  
<sup>d</sup> [goetz.feldmann@rolls-royce.com](mailto:goetz.feldmann@rolls-royce.com), <sup>e</sup> [Ampara.aramcharoen@rolls-royce.com](mailto:Ampara.aramcharoen@rolls-royce.com),  
<sup>f</sup> [chow.wong@rolls-royce.com](mailto:chow.wong@rolls-royce.com)

**Keywords:** Cold Work, Electron Back-Scatter Diffraction, Residual Stress, RR1000, Surface Strengthening, X-Ray Diffraction

**Abstract.** A novel mechanical surface treatment has been investigated for its ability to introduce compressive residual stresses as well as low cold work and surface roughness to metallic components, all of which are known to contribute to fatigue performance enhancement. Comprehensive evaluation of the surface integrity is therefore crucial for surfaces of load bearing components where fatigue life is a concern. The novel treatment involves submerging a work piece within a vibratory chamber filled with hardened stainless steel media, analogous to the mass finishing process. During the treatment, the work piece's surface is peened and polished simultaneously through the normal and shear stresses generated by impacts between the work piece and steel media. The surface integrity generated by this treatment is intimately related to the processing parameters. This work focuses on measurements of residual stresses and cold work distribution in the near-surface layers as well as surface topography generated at different stages of processing. Such measurements allow for process optimisation as well as a better understanding on the contribution of the different aspects of surface integrity to mechanical performance, particularly fatigue.

## Introduction

Residual stresses and surface integrity are known to influence fatigue performance of metallic alloys [1,2]. Tensile residual stresses are known to be undesirable as they promote the propagation of fatigue crack resulting in a fatigue debit (i.e. reduction in life before failure) [1]. Compressive residual stresses on the other hand are desirable for fatigue life enhancement [3,4]. Various surface treatments have therefore been developed with the aim of delivering desirable compressive residual stresses near the free surface where fatigue cracks are typically initiated [5].

The novel surface strengthening being investigated in the current work aims to introduce desirable compressive residual stresses while also reducing surface roughness and the amount of cold work in sub-surface layers. All of these are postulated to generate fatigue performance improvements.

## Experimental methods

**Materials.** The material being investigated in the current work is a nickel based superalloy RR1000 manufactured through a powder metallurgy route (see Table 1 for chemical composition). The alloy is typically utilised in the hot section of aero-engines for its excellent mechanical properties at elevated temperatures.

Table 1: Chemical composition of RR1000 (weight %, balance nickel) [6]

Co	Cr	Mo	Al	Ti	Ta	Hf	C	B	Zr
18.5	15	5	3	3.6	2	0.5	0.027	0.015	0.055

Plain rectangular specimens of RR1000 (80 x 20 x 10 mm) were machined from a forged disc after solution heat treatment and age homogenisation. Heat treatments were applied to the alloy as a means to control the grain size. Coarse (approximately 25-60 μm) grain size microstructures were developed by employing a controlled heat treatment process. Different grain sizes can be developed to optimise the alloy’s performance according to its operating conditions. The coarse grain microstructure being investigated here is optimised for its high temperature performance as it is less susceptible to creep deformations. Fly-cutting was employed as the final machining process to generate a surface integrity typically seen on the nickel disc components manufacturing. Three distinct processing routes were applied to the specimens, as summarised in Fig. 1. Brief descriptions of the different processes involved are shown in the following sections.

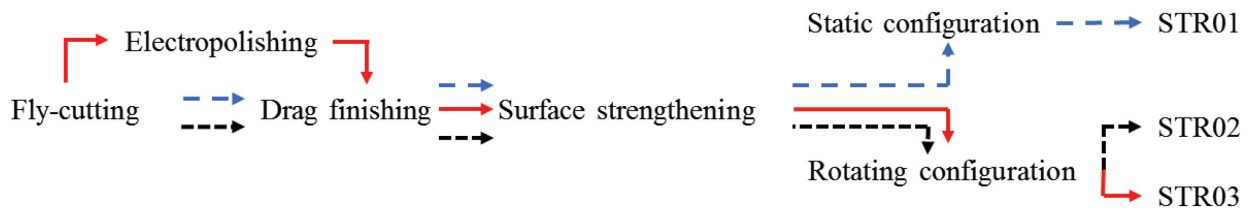


Figure 1: Processing routes applied to the specimens being investigated in this work

**Drag finishing.** Drag finishing aims to remove burrs generated during fly-cutting. All specimens were drag finished where they were rotated at a controlled speed through a wet mixture of SiC cutting chips/media while being held stationary with respect to the rotary spindle. MultiFinish MFD500 was utilised to complete the drag finishing process, with an immersion depth and rotation speed of 220 mm and 100 RPM respectively. The spindle was programmed to change its rotational direction (clockwise/anti-clockwise) every 5 minutes during the entire processing time of 30 minutes.

**Surface strengthening.** A novel surface strengthening process that generates desirable surface finish as well as compressive residual stresses has been jointly developed with Rolls-Royce. During the process, the specimens were rigidly fixed to a structure connected to the vibratory trough filled with stainless steel media with either no movement (static configuration) or rotational movement (rotating configuration) allowed during the process. The vibration generated by the trough produced kinetic agitation of the steel media. When these agitated media come into contact with the surface of the specimen, some of the kinetic energy from the media is used to introduce plastic deformation on the specimens’ surface. Several possible configurations of the process have been studied previously [7-10] and were found to generate promising results. The surface strengthening process covered in this work was completed using a Walther Trowal TMV175/85VP vibratory trough. Details of the media geometry and surface treatment parameters are Rolls-Royce’s proprietary information and are thus omitted from this publication.

**Characterisation.**

**Residual stresses.** In all stress measurements, manganese radiation ( $\lambda = 2.1031\text{\AA}$ ) at 30 kV and 6.7 mA was used to acquire the {311} diffraction peak at 2 $\theta$  angle of around 156°. This particular lattice plane was found to be representative of the bulk property of the  $\gamma/\gamma'$  structure. The Young’s modulus and Poisson’s ratio of the alloy used for the {311} reflection are 220 GPa and 0.300 respectively. All measurements were carried out using Stresstech Xstress G3 X-Ray Diffraction (XRD) equipment with an averaged depth of penetration of approximately 5 μm.

$\text{Sin}^2\psi$  measurements were performed at  $\psi$  offsets between  $-36^\circ$  and  $39^\circ$ . Linear regressions were performed on the acquired  $d$  vs  $\text{Sin}^2\psi$  data to determine the residual stress. Readers are directed to EN15305, which all residual stress measurements performed in this work follow for further details on the methodology. XRD Measurements were carried out in the transverse direction, along the width of the sample.

Layer removal technique is necessary to generate the residual stress profile over the depth of the sample due to limited X-ray penetration. The surface layer was successively removed through electro-polishing. A stylus profilometer was employed to measure the depth of the layer removed through electro-polishing using a step-height measurement. A number of measurements at various layer depths were completed for each specimen in order to observe the variation of residual stress with depth under the free surface. No correction factors were applied for residual stresses measurements in the sub-surface as the layers removed were small relative to the thickness of the sample.

**Areal topography.** Areal topography measurements were completed using an optical system, Taylor Hobson CCI white light interferometry (WLI), with  $20\times$  objective lens and field of view of approximately  $900$  by  $900$   $\mu\text{m}$ . The raw data was then filtered using a Robust Gaussian filter with a prescribed cut-off wavelength of  $800\mu\text{m}$  to eliminate waviness from the parameters computation. All parameters were then computed using TalyMap Gold software while ensuring compliance to the prevailing standards for areal topography characterisation, ISO25178.

**Cold work.** Electron Backscatter Diffraction (EBSD) technique has been used as a tool to estimate cumulative plastic strain using different available metrics based on local misorientations [11] and its usefulness has been demonstrated for evaluation of mechanically treated surfaces using grain orientation spread (GOS) [12]. GOS describes the average deviation in orientation between individual point in a grain and that of the grain to evaluate plastic strain within the material. High GOS values are related to high degree of plastic deformation (i.e. cold worked) and vice versa. Using a statistical analysis, an estimate of the depth of the cold worked or deformed zone can be obtained. The data can also be displayed visually using orientation imaging microscopy (OIM) to show maps of scanned areas.

EBSD is particularly sensitive to the surface topography as the diffraction signal comes from the top few nanometres of the crystal lattice. The cross-sectioned surface was first of all polished using 1200 grit SiC paper before ion-milled to remove  $25$   $\mu\text{m}$  of material layer using JEOL cross sectional polisher followed by a short surface ion-milling to ensure a good surface topography for EBSD mapping. EBSD mapping was completed over an area of  $250$  by  $250$   $\mu\text{m}$  with a step size of  $0.3$   $\mu\text{m}$  using an Oxford EBSD detector – NordlysMax. The acceleration voltage and tilt angle used during the EBSD mapping were  $20$  kV and  $70^\circ$  respectively.

Ignoring the effects of low-angle grain boundaries and other microstructural features, full-width at half maximum (FWHM) obtained from the peak broadening can also be utilised to estimate the amount of cold work using an appropriate calibration curve [13].

## Results

Surface topography is commonly characterised using the arithmetic roughness average ( $S_a$ ) parameter. From Fig. 2, it can be observed that the averaged roughness is reduced from  $0.63$   $\mu\text{m}$  after fly-cutting to  $0.43$   $\mu\text{m}$  after drag finishing and finally to  $0.29$   $\mu\text{m}$  after surface strengthening. The regular structure of the topography was also observed to diminish with surface treatment particularly the surface strengthening process. This reflects the random nature of the media collision with the specimen's surface. The final topography is expected to be favourable for the fatigue performance.

Residual stress depth profiles obtained from XRD measurements are shown in Fig. 3. The measurements were completed on specimens at different stages of surface treatment: as-machined (AM), as-machined & drag finished (DF), electropolished (EP), electropolished & drag finished (EPDF) and surface strengthened (STR01-03, refer to Fig. 1).

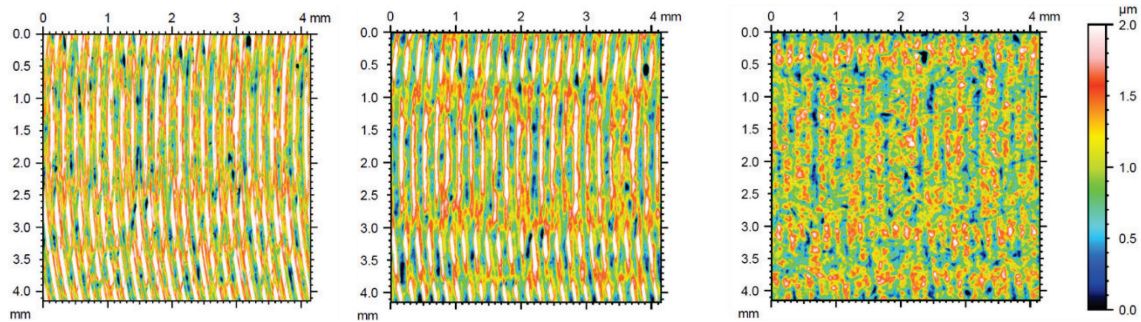


Figure 2: Surface topography changes from as-machined (left) to drag finished (middle) and surface strengthened, STR01 (right)

Fig. 4 shows the grain orientation spread (GOS) maps obtained from the EBSD analysis on coarse grain samples. Regions with low cold work are shown in blue where GOS value is low. It can be seen that the as-machined surface (Fig. 4a) has a certain degree of cold work and further processes (drag finishing (Fig. 4b) and mechanical surface strengthening (Fig. 4d-e)) were not found to result in observable reduction in cold work. Electropolishing (approx. 160 μm of material removal) on the other hand was found to be capable of removing virtually all the cold worked layer. Drag finishing applied to the electropolished surface was not found to introduce appreciable cold work (Fig. 4c). Comparing the GOS maps obtained from surface strengthened specimens, STR03 was found with the least amount of cold work (Fig. 4f). The results shown in the GOS maps are consistent with the full-width at half maximum values obtained from the XRD measurements at the surface (see Table 2).

Table 2: Full-width at half maximum (FWHM) readings and the corresponding estimated cold work obtained from different samples at the surface taken from the transverse direction.

Sample	AM	DF	EP	EPD F	STR0 1	STR0 2	STR0 3
FWHM (°)	6.55± 0.2	5.77± 0.1	2.72± 0.3	4.45± 0.1	4.91± 0.2	5.77± 0.2	4.43± 0.1
Cold work (%)	48.5	37.7	5.6	21.8	27.0	37.7	21.6

### Discussions

High tensile stresses observed at the as-machined surface are not unusual for nickel based superalloys as large amount of heat can be accumulated at the surface during the cutting operation due to the alloy's low thermal conductivity. The tensile residual stress layers are compensated by the compressive residual stress layers, extending up to 180 μm deep in the coarse grain example.

Drag finishing only influenced residual stresses at the surface without generating significant impact on the sub-surface residual stresses, perhaps due to the insignificant material removal by the process (< 1 μm). The surface strengthening process was found to induce desirable compressive residual stresses to the material as evident from the residual stress profiles being dominated by compressive stresses after the surface strengthening process.

Electropolishing was found to be capable of removing the tensile stressed layers generated from the fly-cutting. Drag finishing after electropolishing was observed to imbue compressive stresses in the thin layer near the surface (approximately < 20 μm).

Interestingly, the final residual stress profiles after surface strengthening (i.e. STR01-03) are largely similar despite the observed variations in the residual stresses prior to the surface strengthening treatment. The final cold work at the surface on the other hand was observed to be sensitive to the processes prior to the strengthening treatment. When the degree of cold working is high prior to the strengthening treatment, the final cold work after strengthening tend to also be high

and vice versa. Minimal degree of cold work is desired for improved high temperature fatigue performance as high degree of cold work has been linked to increase in the relaxation of compressive residual stresses [14]. Therefore it is important to optimise the processes prior to the strengthening treatment in order to minimise the degree of cold working on the surface.

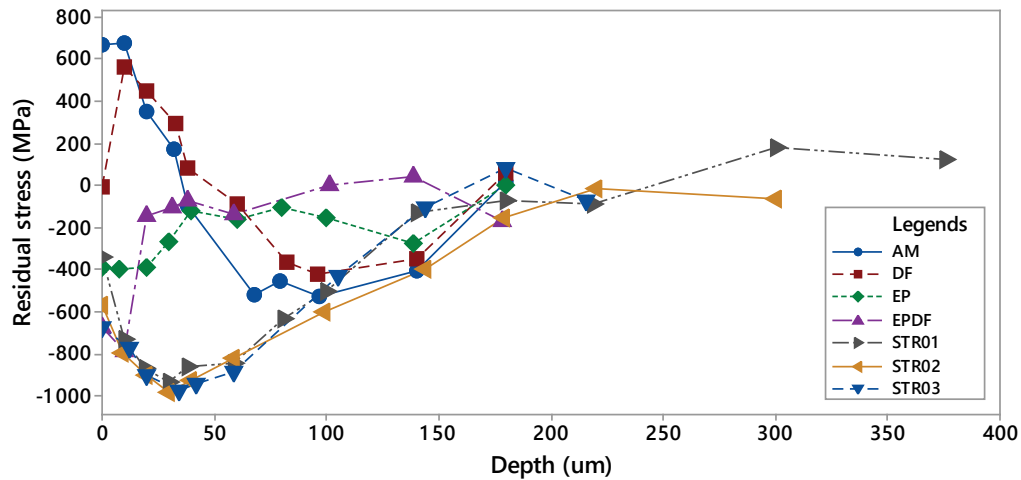


Figure 3: Residual stress depth profiles for coarse grain specimens.

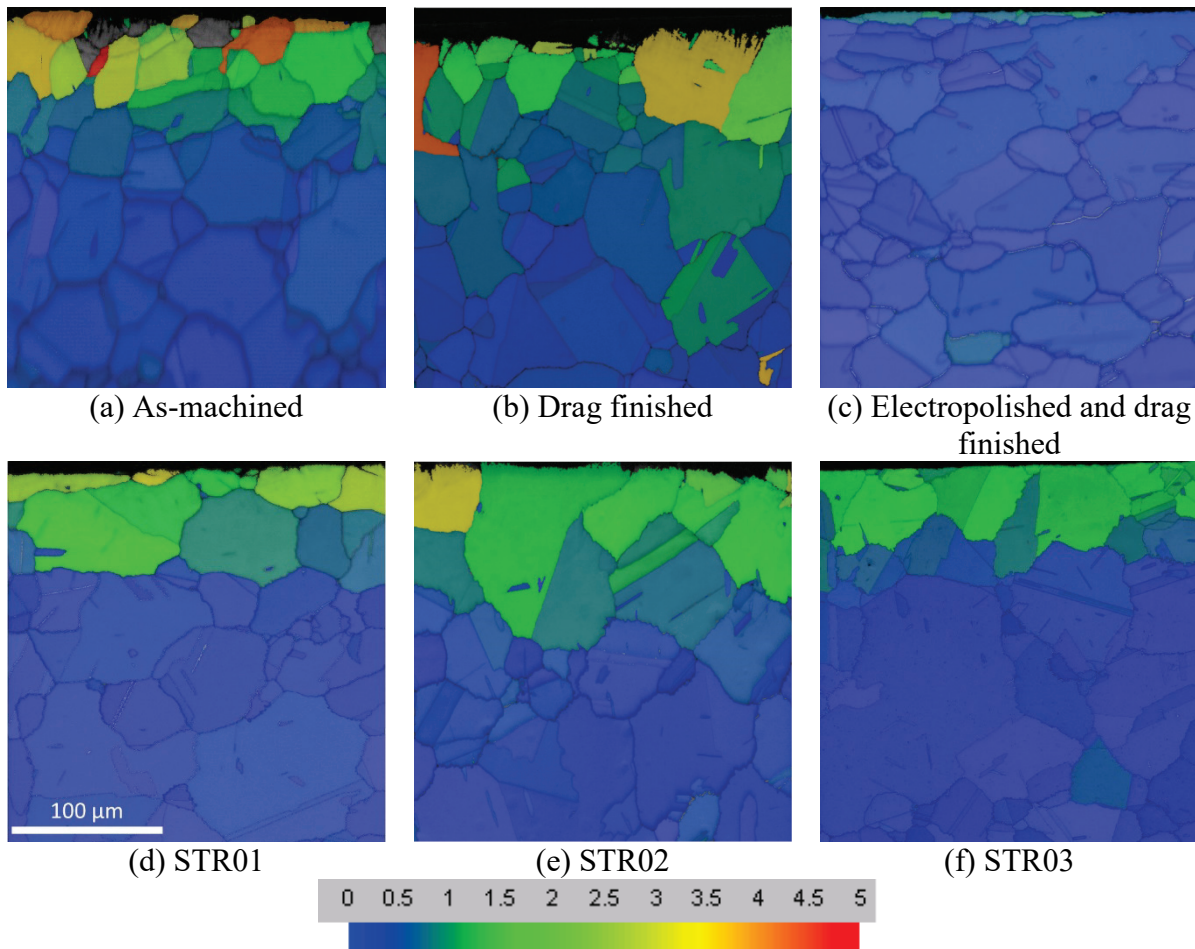


Figure 4: Grain orientation spread (GOS) maps for coarse grain RR1000 specimens. All images were obtained at the same magnification thus the scale bar on (d) is applicable to all maps.

## Conclusions

The novel mechanical surface strengthening process was found to be capable of introducing desirable compressive stresses, but it has only a limited influence on the final amount of cold work (based on FWHM). It is therefore crucial to ensure that the cold work is removed prior to the strengthening treatment. A gentle finishing process such as electropolishing was found to be effective for cold worked layers removal. Such processes can potentially be employed before the mechanical strengthening process to generate a final surface with desirable compressive residual stresses whilst minimising the amount of cold work being introduced into the material to optimise its fatigue performance.

## References

- [1] D. Novovic, R. C. Dewes, D. K. Aspinwall, W. Voice and P. Bowen, The effect of machined topography and integrity on fatigue life, *Int. J. Machine Tools & Manufacture* 44 (2004) 125-134. <http://dx.doi.org/10.1016/j.ijmachtools.2003.10.018>
- [2] D. T. Ardi, Y. G. Li, K. H. K. Chan, L. Blunt and M. R. Bache, Surface topography and the impact on fatigue performance, *Surface Topography Metrology and Properties* 3 (2015) no. 1.
- [3] L. Wagner, Mechanical surface treatments on titanium, aluminium and magnesium alloys, *Materials Science and Engineering A* 263 (1999) 210-216. [http://dx.doi.org/10.1016/S0921-5093\(98\)01168-X](http://dx.doi.org/10.1016/S0921-5093(98)01168-X)
- [4] K. A. Soady, Life assessment methodologies incorporating shot peening process effects: mechanistics consideration of residual stresses and strain hardening part 1, *Materials Science and Technology* 29 (2013) no. 6.
- [5] V. Schulze, *Modern mechanical surface treatment: States, Stability, Effects*, Wiley, 2005. <http://dx.doi.org/10.1002/3527607811>
- [6] M. C. Hardy, C. Herbert, J. Kwong, W. Li, D. A. Axinte, A. R. C. Sharman, A. Encinas-Oropesa and P. J. Withers, Characterising the integrity of machined surfaces in a powder nickel alloy used in aircraft engines, *Procedia CIRP* 13 (2014) 411-416. <http://dx.doi.org/10.1016/j.procir.2014.04.070>
- [7] G. G. Feldmann and T. Haubold, Mechanical surface treatment technologies for improving HCF strength and surface roughness of blisk rotors, *Materials Science Forum* 768-769 (2013) 510-518. <http://dx.doi.org/10.4028/www.scientific.net/MSF.768-769.510>
- [8] G. Feldmann, W. Wei, T. Haubold and C. C. Wong, Application of vibropeening on aero-engine component, *Procedia CIRP* 13 (2014) 423-428. <http://dx.doi.org/10.1016/j.procir.2014.04.072>
- [9] M. D. Sangid, J. A. Stori and P. M. Ferreira, Process characterization of vibrostrengthening and application to fatigue enhancement of aluminum aerospace components - Part I. Experimental study of process parameters, *Int. J. Adv. Manufacturing Technology* 53 (2010) 545-560. <http://dx.doi.org/10.1007/s00170-010-2857-2>
- [10] M. D. Sangid, J. A. Stori and P. M. Ferreira, Process characterization of vibrostrengthening and application to fatigue enhancement of aluminum aerospace components - Part II: Process visualisation and modelling, *Int. J. Adv. Manufacturing Technology* 53 (2011) 461-575. <http://dx.doi.org/10.1007/s00170-010-2858-1>
- [11] M. Kamaya, A. J. Wilkinson and J. M. Titchmarsh, Quantification of plastic strain of stainless steel and nickel alloy by electron backscatter diffraction, *Acta materialia* 54 (2006) 539-548. <http://dx.doi.org/10.1016/j.actamat.2005.08.046>
- [12] D.J.Child, G.D.West and R.C.Thomson, Assessment of surface hardening effects from shot peening on a Ni-based alloy using electron backscatter diffraction techniques, *Acta Materialia* 59 (2011) 4825-4834. <http://dx.doi.org/10.1016/j.actamat.2011.04.025>
- [13] W.Li, P.J.Withers, D.Axinte, M.Preuss and P.Andrews, Residual stresses in face finish turning of high strength nickel-based superalloy, *J. Mat. Processing Technology* 209 (2009) 4896-4902. <http://dx.doi.org/10.1016/j.jmatprotec.2009.01.012>
- [14] P.S.Prevey, The effect of cold work on thermal stability of residual compression in surface enhanced IN718, *Metal Finishing News* 6 (2005).